An update to this article is included at the end

Results in Chemistry 2 (2020) 100026

Contents lists available at ScienceDirect

Results in Chemistry

journal homepage: www.elsevier.com/locate/rechem

Characterization of an aryl piperazine/2-hydroxypropyl-β-cyclodextrin association, a complex with antidiabetic potential

R. Devine [a], D.S.D. Martin [b], G.K. Kinsella [d], J.B.C. Findlay [b,e], J.C. Stephens [a,c,*]

[a] Department of Chemistry, Maynooth University, Maynooth, Co. Kildare, Ireland
[b] Department of Biology, Maynooth University, Maynooth, Co. Kildare, Ireland
[c] The Kathleen Lonsdale Institute of Human Health Research, Maynooth University, Maynooth, Co. Kildare, Ireland
[d] School of Food Science and Environmental Health, College of Sciences and Health, Technological University Dublin, Dublin D07 ADY7, Ireland
[e] School of Biomedical Sciences, University of Leeds, Leeds, UK

ARTICLE INFO

Article history:
Received 23 November 2019
Accepted 30 December 2019

Keywords:
Diabetes
Aryl piperazine
2-Hydroxypropyl-β-cyclodextrin

ABSTRACT

This study explores the molecular association between 4-(thiophen-2-yl)-1-(4-(4-(trifluoromethyl)phenyl) piperazin-1-yl)butan-1-one (RTC1), an antidiabetic compound recently reported by our research group with challenging aqueous solubility, and 2-hydroxypropyl-β-cyclodextrin (HPBCD). The formation of a RTC1/HPBCD complex resulted in improved solubility. A phase-solubility diagram was used to determine the complex stability constant and stoichiometric ratio. 2D ^{1}H NMR spectroscopy was utilized to study the molecular interaction between RTC1 and HPBCD in the complex. Differential scanning calorimetry and scanning electron microscopy was also employed to confirm complex formation. In vitro biological evaluation, using a glucose uptake assay, showed that the homogeneous RTC1/HPBCD complex solution showed the same activity to that of RTC1 alone, with no reduction in activity due to the presence of HPBCD.

© 2020 Published by Elsevier B.V. This is an open access article under the CC BY-NC-ND license (http://creativecommons.org/licenses/by-nc-nd/4.0/).

1. Introduction

Type 2 diabetes mellitus (T2DM) is now one of the major modern public health threats in terms of human, social, and economic costs [1]. T2DM is a chronic condition where blood glucose levels are raised due to the body's inability to produce sufficient amounts of insulin or to use insulin effectively. Insulin is produced in the pancreas, is an essential hormone and plays a critical role in the transport of blood glucose into the body's cells. A lack of insulin or a cell's insensitivity to insulin leads to hyperglycaemia where blood glucose levels are elevated, and which, if left unchecked, can result in organ damage and the development of disabling and life-threatening health complications [1,2]. There are a number of T2DM therapeutic options available, some of which can be administered at early stages of disease development or as a combination therapy with injectables. These include metformin, sulfonylureas, thiazolidinediones, dipeptidyl peptidase-4 (DPP-4) inhibitors, sodium-glucose transport protein 2 (SGLT2) inhibitors, Glucagon-like peptide 1 (GLP-1) receptor agonists and insulin, but the control of diabetes remains variable and can be unsatisfactory [2–4]. For some sufferers, the therapeutic regimens, side effects, and possible off-target actions of some options are undesirable and can result in reduced compliance [5–8]. As a consequence and taking into account the projected and rapid growth in the number of those suffering with diabetes, there is an ever-increasing demand for novel anti-diabetic therapies with defined mechanisms of action. Recently, we reported the piperazine containing compounds RTC1 and RTB70, which act through the inhibition of NADH:ubiquinone oxidoreductase (complex I of the mitochondrial respiratory chain) to stimulate glucose uptake and restore the glucose handling abilities of diabetic mice [9]. The reduction in NADH:ubiquinone oxidoreductase activity provoked leads to a change in cellular ADP:ATP and AMP:ATP ratios resulting in the activation of AMP-activated protein kinase (AMPK). Once activated, AMPK rapidly restores cellular energy balance by switching off ATP consuming anabolic pathways and by switching on ATP generating catabolic pathways involving increased glucose uptake [10]. Further studies showed that RTC1 augmented the signalling capabilities of insulin in C2C12 cells stimulated with tumour necrosis factor-alpha (TNF-α), thus preventing TNF-α induced insulin resistance through action as an insulin sensitizer [11]. However, throughout these studies RTC1 showed poor aqueous solubility, which could hamper the subsequent further development of this promising hit compound.

A number of systems exist which can be employed to improve drug bioavailability and solubility, ranging from chemical modifications (e.g. prodrugs, attachment of PEG linkers) to the encapsulation of drugs

* Corresponding author at: Department of Chemistry, Maynooth University, Maynooth, Co. Kildare, Ireland.
E-mail address: john.stephens@mu.ie (J.C. Stephens).

https://doi.org/10.1016/j.rechem.2020.100026
2211-7156/© 2020 Published by Elsevier B.V. This is an open access article under the CC BY-NC-ND license (http://creativecommons.org/licenses/by-nc-nd/4.0/).

within a suitable vehicle (e.g. liposomes, cyclodextrins). These systems work by improving certain properties of a drug, such as premature metabolic degradation or poor water solubility, allowing the drug to reach its target and evoke a pharmacological response [12]. Cyclodextrins (CD) can improve the solubility, stability, and bioavailability of drug molecules through their ability to form a non-covalent inclusion complex [12,13]. Cyclodextrins are chemically formed when glucopyranose molecules are bound together through α-(1–4) bonds. They are most commonly composed of 6 (α-CD), 7 (β-CD) or 8 (γ-CD) glucose units [12]. β-CD appears an attractive choice for many pharmaceutical applications due to its ready availability and the appropriate size of its cavity, allowing for the inclusion of the widest range of drugs [13]. However, its low aqueous solubility and associated nephrotoxicity limits its use [13]. For this reason, modified CDs have been produced. Hydroxylpropyl-β-cyclodextrin (HPBCD) is one such modified CD that is employed for the encapsulation of drug molecules [14]. It has been used in parenteral, oral, transdermal, and ocular drug delivery systems due to its high water solubility and lack of toxicity in vivo [14–16].

The hydrophobic cavity and the hydrophilic exterior of CDs enable these cyclic oligosaccharides to function as efficient drug delivery systems [12,17]. The driving force behind the formation of an inclusion complex is the release of water molecules from the CD cavity, with electrostatic and hydrophobic interactions, van der Waals forces, and hydrogen-bonding all contributing to the inclusion of a drug molecule [18]. The release of a drug molecule occurs as these interactions are relatively weak, which allows the free drug and uncomplexed cyclodextrin to be in equilibrium with the inclusion complex when in solution [18].

The aim of this work was to establish an aqueous CD based solvent system for the dissolution of RTC1 and to study the molecular association that takes place between RTC1 and HPBCD. A phase-solubility diagram and two dimensional proton nuclear magnetic resonance (2D ^{1}H NMR) spectroscopy was performed in order to ascertain inclusion complex formation and to estimate the inclusion mode. Differential scanning calorimetry (DSC) and scanning electron microscopy (SEM) were also employed to allow characterization of the complex in the solid state. Finally, the in vitro ability of the RTC1/HPBCD complex to stimulate glucose uptake in mouse C2C12 cells was determined and compared to RTC1 alone.

2. Results and discussion

RTC1 can be prepared according to our published literature procedure with some minor modifications (Scheme 1 and Supporting information) [9]. A two-step process was employed that utilized S_NAr and coupling reactions (Scheme 1). The aryl piperazine **2** was generated from 4-chlorobenzotrifluoride **1** and piperazine by heating the reaction to 200 °C under microwave conditions (50% yield). Coupling of the resultant **2** with the commercially available 4-(2-thienyl)butyric acid **3** gave the desired RTC1 in 80% yield (Scheme 1).

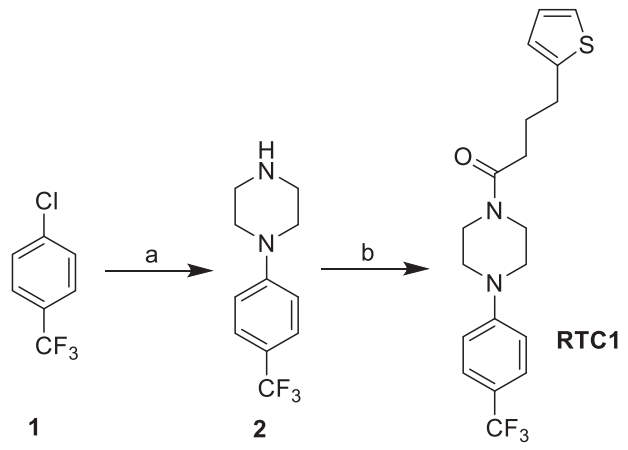

Scheme 1. Synthesis of RTC1. Reagents and conditions: (a) piperazine, NMP, 30 min, 200 °C, MW, 50% yield; (b) 4-(2-thienyl)butyric acid **3**, HOBt, TBTU, NEt_3, DMF, overnight, rt, 80% yield [9].

Table 1
Solubility study for the generation of a 0.02 M RTC1 solution.

% DMSO	HPBCD (eq)	Solubility
0	20	Insoluble
50	1	Insoluble
50	2	Insoluble
50	5	Insoluble
50	10	Insoluble
50	12	Soluble
10	12	Insoluble
10	18	Insoluble
10	20	Soluble
5	20	Soluble
2	20	Insoluble[a]

[a] Was soluble initially but precipitate subsequently appeared.

A solubility study was conducted in order to prepare an aqueous 0.02 M solution of RTC1 using HPBCD as a complexing agent. The first attempt involved the use of 20 equivalents of HPBCD in 100% water. However, this did not result in the dissolution of RTC1. We then explored the use of DMSO as a co-solvent, in combination with HPBCD, where a number of variations were explored (Table 1). DMSO was chosen due to its low toxicity, but also experimental studies in the formation of inclusion complexes have suggested that stable inclusion complexes can be formed in the presence of DMSO [19]. The results of this study are summarized in Table 1, where the use of up to 50% DMSO still resulted in insolubility, however the combination of 5% DMSO with 20 equivalents of HPBCD produced a homogeneous solution and was considered optimal. The solubilising effect of HPBCD can be seen in Fig. 1. We suggest that the resultant homogeneous solution of RTC1 was due, in part, to the formation of an inclusion complex. To characterize this inclusion complex, a number of analytical techniques were employed, namely a phase solubility diagram, NMR spectroscopy, DSC, and SEM.

The Higuichi and Connors method for phase-solubility diagrams was employed to explore the effect of HPBCD on the aqueous solubility of RTC1 (see Supporting information) [20]. As can be seen in Fig. 2, the solubility of RTC1 increases linearly with increasing concentrations of HPBCD, and hence is an A_L type solubility curve, which indicates the presence of a water soluble complex. This is the most common complex observed for drug:CD interactions [14]. The slope, of value 0.012 in this case, is less than one and suggests the presence of a complex with a 1:1 stoichiometry [20].

The apparent stability constant ($K_{1:1}$) was estimated according to Eq. (1), where *So* is the intrinsic water solubility of the drug and the

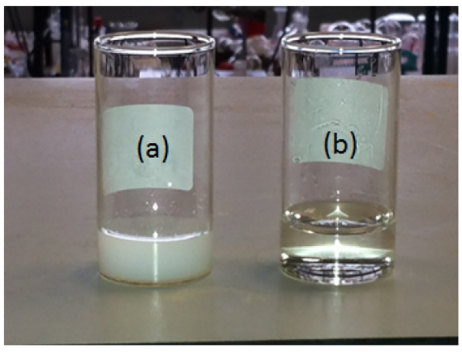

Fig. 1. (a) RTC1 in a 5% DMSO/H_2O solution without HPBCD. (b) RTC1 in a 5% DMSO/H_2O solution with 20 equivalents of HPBCD.

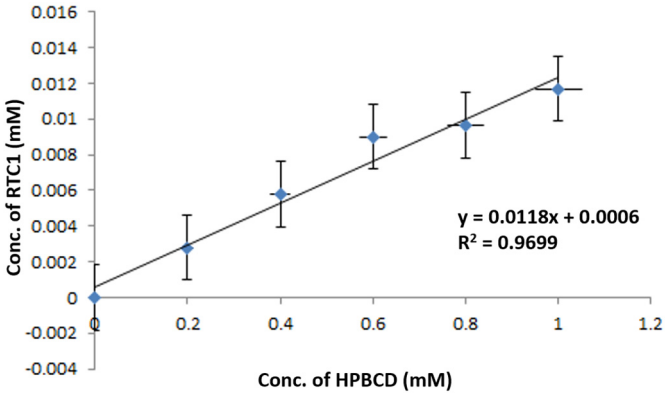

Fig. 2. Phase solubility diagram for RTC1/HPBCD host-guest system at rt.

Table 2
Chemical shifts for free RTC1 and RTC1/HPBCD complex.

Assignment (RTC1)	δ[a] (free RTC1)	δ[a] (RTC1/HPBCD complex)	Δδ
H2, H4	7.0904	7.0784	0.0120
H6	2.5184	2.5078	0.0106
H8	2.9384	2.9289	0.0095
H10	6.8687	6.8621	0.0066
H11	6.9540	6.9465	0.0075

[a] δ in ppm.

slope is the slope of the line generated from the phase-solubility diagram [14].

$$K_{1:1} = \frac{\text{Slope}}{\text{So}(1-\text{Slope})} \quad (1)$$

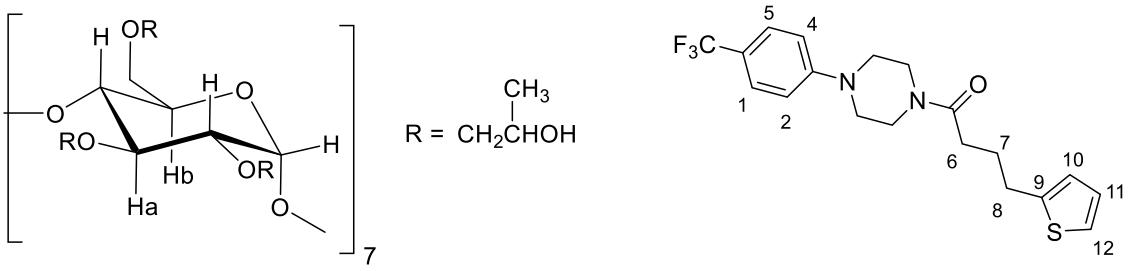

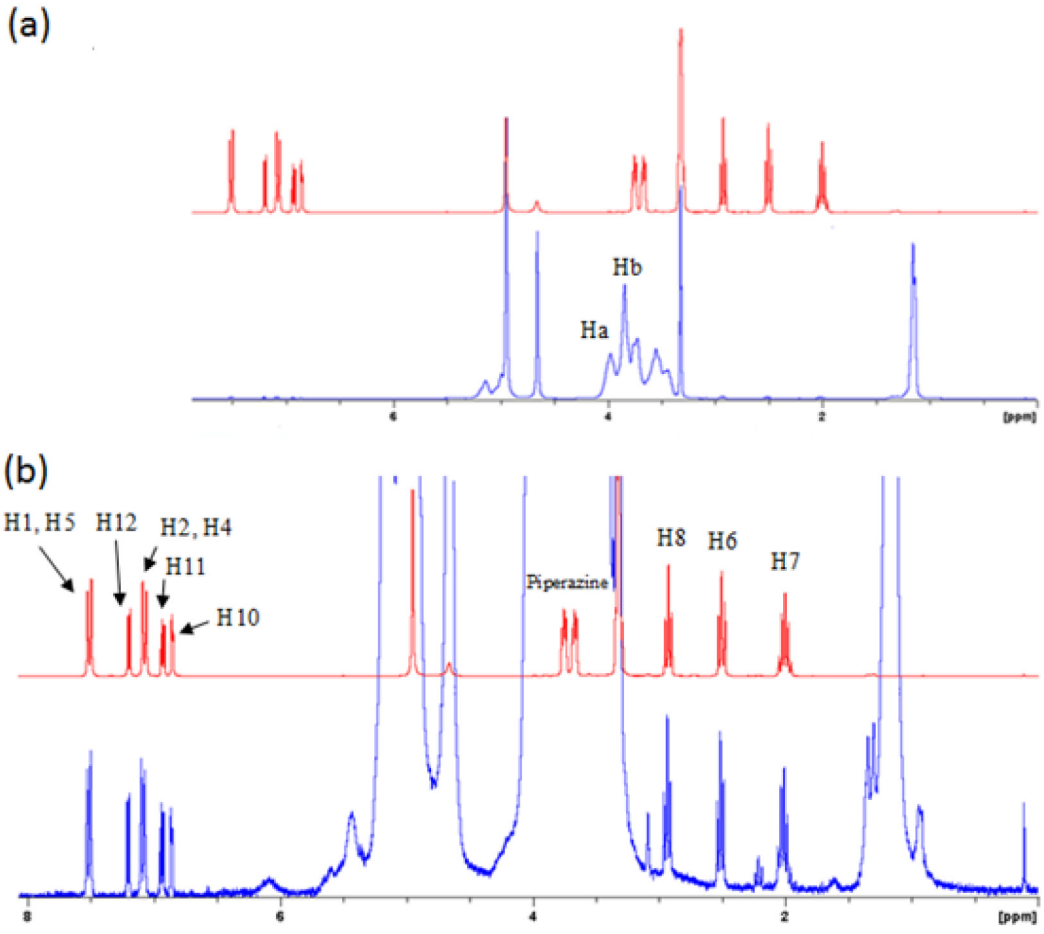

Fig. 3. ^{1}H NMR spectra (300 MHz) in 5% D_2O/CD_3OD of (a) RTC1 (red) and the inclusion complex (blue) and (b) a magnified view of the spectrum.

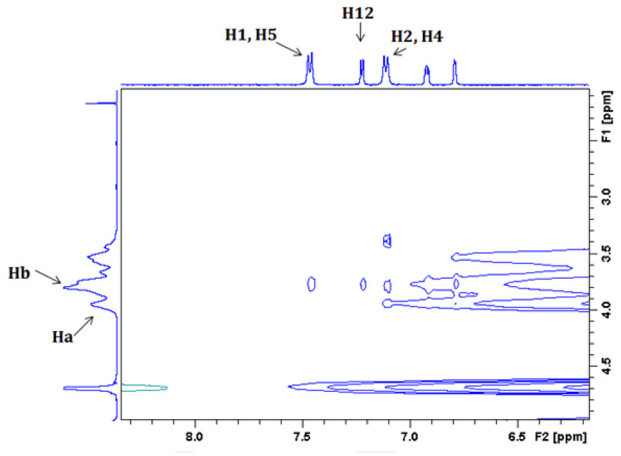

Fig. 4. ROESY spectrum showing the crosspeaks between the aromatic signals of the inclusion complex between RTC1 and HPBCD protons.

The intrinsic water solubility (0.32 μM) was calculated using UV-spectroscopy (see Supporting information). Using Eq. (1), $K_{1:1}$ was calculated to be 34,755 M^{-1}. The value of $K_{1:1}$ is a useful index to estimate the degree of binding strength of the complex. Here, the $K_{1:1}$ is an approximate value ($R^2 = 0.9699$) and can be compared to that reported by Upadhye et al. who described a binding constant of 21,137 M^{-1}, which indicated a strong bonding interaction between the drug molecule Δ^9-tetrahydrocannabinol (THC) and a CD [15]. Upadhye also gave an example of a drug molecule which formed weak, unstable interactions within a CD molecule. In this case the molecule, Δ^9-tetrahydrocannabinol hemisuccinate (THC-HS), a prodrug derivative of the previously mentioned THC, was found to have a $K_{1:1}$ value of 562.48 M^{-1} [15]. The large stability constant value obtained for RTC1 suggests a favourable interaction between the molecule and HPBCD, with the equilibrium lying in favour of the inclusion complex. Although the phase diagram suggested the formation of a RTC1/HPBCD complex with a 1:1 stoichiometry, 20 equivalents of HPBCD was still required to form a homogeneous solution. This is to be expected, for as explained by Rojas-Aguirre et al., a phase solubility diagram can indicate the presence of a complex with a 1:1 stoichiometry, where the level of complexation can be low and excess CD is needed to fully dissolve the required concentration of drug [12]. In addition, the use of excess amounts of CD can achieve solubilisation of drug molecules by the formation of non-inclusion complexes [21]. Gabelica et al. reported that CD can form both inclusion and non-inclusion complexes with certain molecules and that both complexes can exist simultaneously in aqueous solutions [22]. These non-inclusion complexes arise due to the formation of aggregates consisting of two or more CD molecules and drug/CD complexes. The water soluble aggregates can then function to further solubilise lipophilic drugs through the formation of a non-inclusion complex by creating a hydrophobic environment in which to accommodate the drug. Alternatively, Loftsson et al. suggested that solubilisation may also occur through the formation of a micelle like structure [21]. The formation of these non-inclusion complexes may apply to the preparation of the homogeneous 0.02 M solution of RTC1 in 5% aqueous DMSO. As was reported by Loftsson, these non-inclusion complexes occur when a high concentration of drug is present [21]. Therefore, the preparation of a 0.02 M solution of RTC1 may have required 20 eq of HPBCD to allow the formation of, not only the 1:1 inclusion complex, but also the non-inclusion complex formed by the presence of a CD:inclusion complex aggregate [21].

^{1}H NMR spectroscopic analysis was used to investigate the binding mode of RTC1 within HPBCD. The encapsulation of RTC1, either by one molecule of HPBCD or by the formed aggregates, can be seen by changes in the 1D ^{1}H NMR spectra of RTC1 for the inclusion complex. Full characterization of the RTC1/HPBCD complex in D_2O was not possible, as RTC1 could not be solubilised in this solvent. Therefore, a 5% D_2O/CD_3OD solution was prepared in which both RTC1 and the complex were independently soluble. This gave the spectra below where the characteristic peaks of RTC1 were observed within the CD complex (Fig. 3(b), blue spectrum).

A shift in the resonance of a number of peaks for RTC1 was observed and the difference in chemical shift is shown in (Table 2). This indicates that RTC1 is in a different environment when it is present in the CD inclusion (or non-inclusion) complexes. These small changes in chemical shifts are common, with Rojas-Aguirre et al. reporting changes in chemical shifts ranging from 0.001 ppm to 0.012 ppm in their study [12]. The information on the spatial proximity of RTC1 in the CD complexes was determined by means of two-dimensional rotating frame NOE spectroscopy (ROESY). The 2D ROESY spectrum was also obtained using a 5% D_2O/CD_3OD solution with the contour plot revealing an interaction between H1, H2, H3, H4, H5 and H12 of RTC1 with the internal protons Ha and Hb of HPBCD, which were assigned by Rojas-Aguirre et al. (Fig. 4) [12]. This suggests the presence of RTC1 within the cavity of HPBCD, supporting the formation of an inclusion complex.

The thermoanalytical technique, DSC, was also used to study the presence of the inclusion complex. The thermal behaviour of the inclusion complex was compared to that of RTC1, HPBCD, and a physical mixture of RTC1 and HPBCD (see Supporting information). The DSC curve, Fig. 5(a), for RTC1 shows a sharp endothermic peak at 94 °C, which is characteristic of the melting point of RTC1. Fig. 5(b), the curve for HPBCD, is in accordance with the literature and shows two broad endotherms ranging from 25 to 103 °C, due to the loss of water, and 280 to 340 °C, due to decomposition of the CD [12,14]. The physical mixture shows the characteristic peaks of both RTC1 and HPBCD, with the sharp peak at 94 °C due to the melting of RTC1 and the broad endotherm ranging from 25 to 103 °C showing the loss of water from the HPBCD cavity (Fig. 5(c)). This indicates the absence of any interaction between RTC1 and HPBCD [12]. The inclusion complex, Fig. 5(d), has a broad endotherm at 25–103 °C due to the loss of water. Work by Rojas-Aguirre has suggested that this is the loss of water molecules which are bound to the —OH groups on the exterior of the CD and not the loss of water from the cavity [12]. The sharp, endothermic peak observed at 94 °C, in the DSC curve of RTC1 and the physical mixture is notably absent from the DSC curve of the inclusion complex. This again suggests the presence of a complex, whether it is an inclusion or non-inclusion complex [21].

An investigation using SEM analysis was employed and compared the shape and surface morphologies of HPBCD, RTC1, the physical mixture, and the RTC1/HPBCD complex. Fig. 6 shows the SEM images for HPBCD, RTC1, the physical mixture, and the RTC1/HPBCD complex at 500 magnifications. HPBCD and RTC1 show distinct morphologies, with RTC1 appearing to adopt a cluster like arrangement in the micrograph. The SEM image of the physical mixture (Fig. 6(c)) has a morphology comparable to that of both RTC1 and HPBCD. The characteristic clusters observed in the micrograph of RTC1 and the smooth morphology of HPBCD can be seen. The morphology of the RTC1/HPBCD complex is clearly different from that of the physical mixture and RTC1. Fig. 6(d), the RTC1/HPBCD complex, shows a smooth solid, without the cluster like structures observed in the SEM image of RTC1.

The in vitro biological activity of the RTC1/HPBCD complex was investigated using a glucose uptake assay. This was to elucidate whether the complexation of RTC1 with HPBCD would hinder its ability to evoke a biological response. As the stability constant was large ($K1:1 = 34{,}755\ M^{-1}$), it was possible that the concentration of free drug would be too low to evoke a response. The assay was performed as previously described, using 10 μM of RTC1 (see Supporting information) [9]. The results, shown in Fig. 7, indicate that the binding of RTC1 in the HPBCD did not affect the compounds ability to stimulate glucose uptake. Although the stability constant was large, indicating the presence of significant interactions within the inclusion complex, it is still

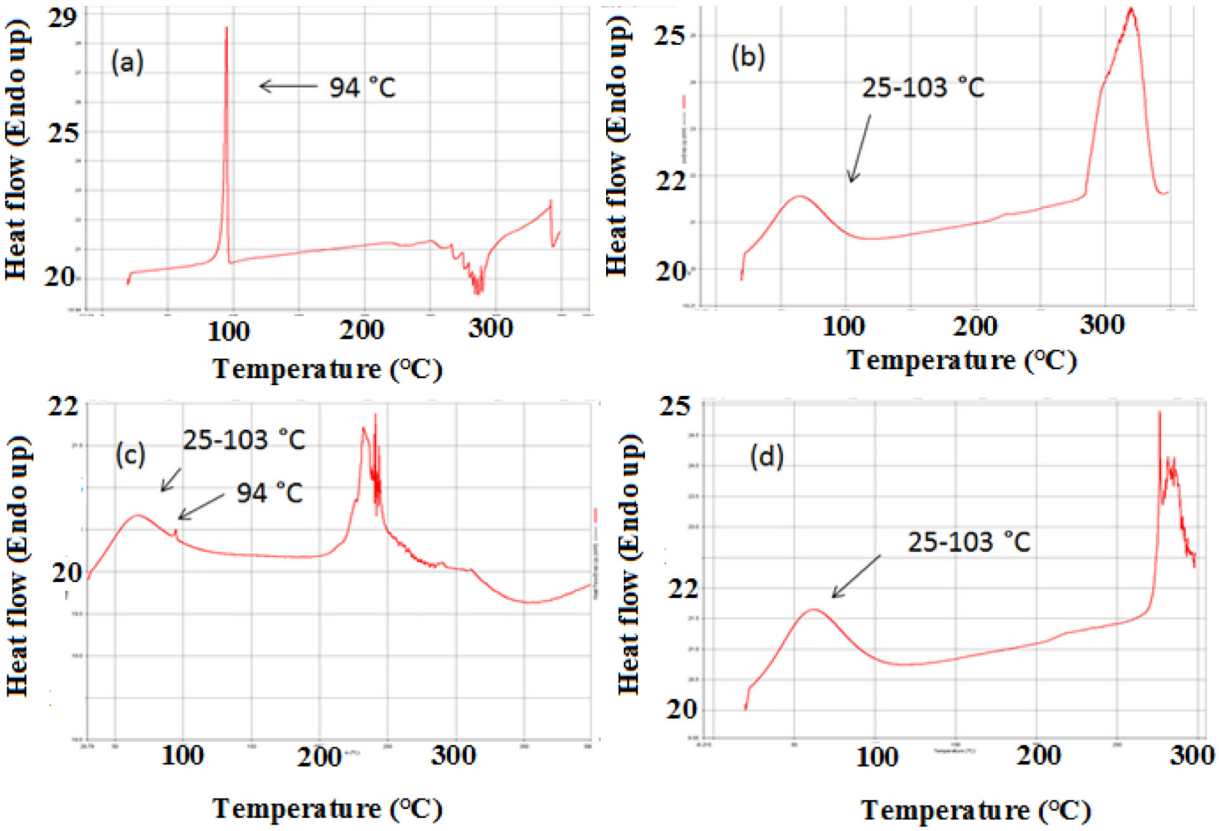

Fig. 5. DSC curves: (a) RTC1 (b) HPBCD (c) physical mixture (d) RTC1/HPBCD complex.

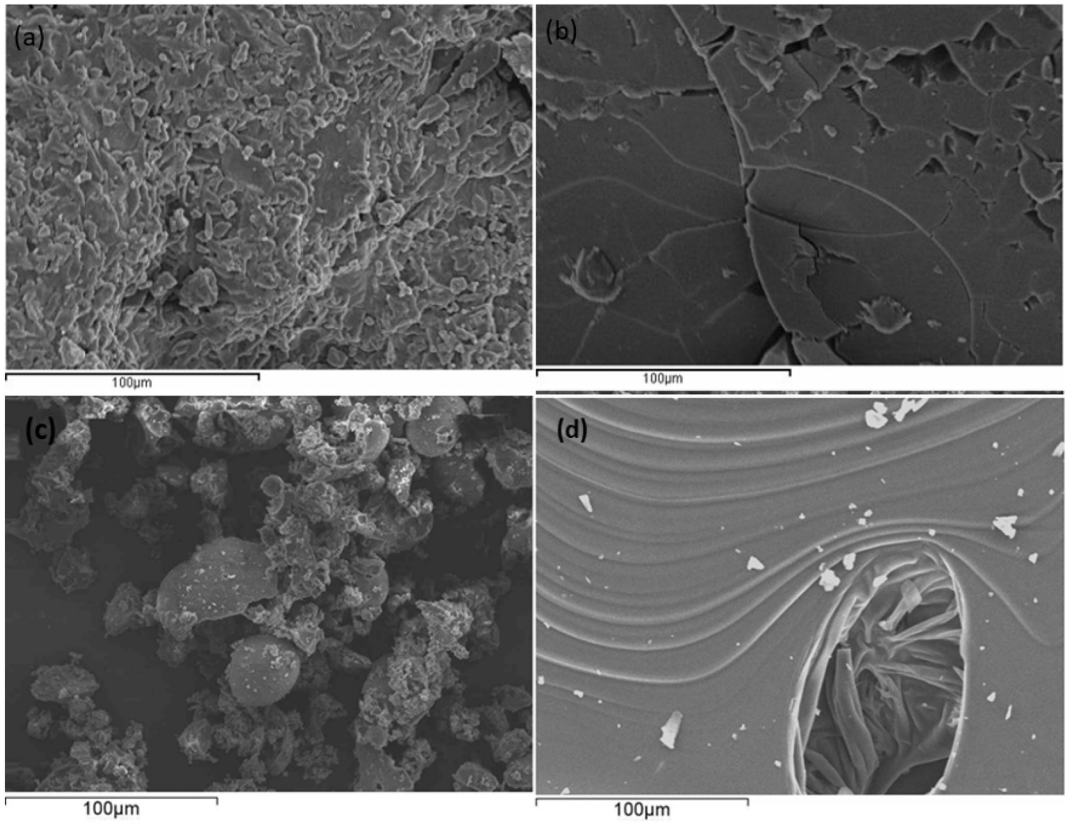

Fig. 6. SEM images (20 kV) of (a) RTC1 (b) HPBCD (c) physical mixture of RTC1 and HPBCD (d) RTC1/HPBCD complex at 500× magnification.

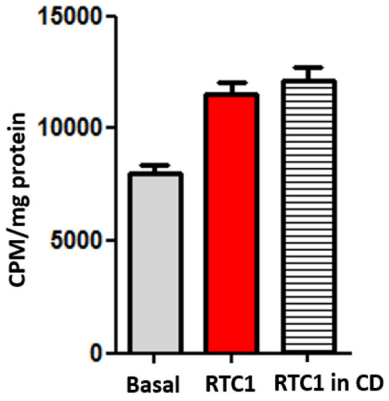

Fig. 7. Glucose uptake assay results for the RTC1/HPBCD complex. 10 μM RTC1 used with 20 eq of HPBCD. C2C12 muscle cells incubated overnight at 37 °C. Cells subsequently exposed to ^{3}H deoxy-2-glucose for 10 min and a scintillation count of the C2C12 muscle cells performed. Values are mean ± S.E.M.; n = 3 (see Supporting information).

possible for RTC1 to become disassociated from the CD and reach the target protein.

3. Conclusion

A convenient method for improving the aqueous solubility of RTC1 was identified with the use of the excipient HPBCD. The enhanced aqueous solubility is likely due to the formation of a RTC1/HPBCD inclusion complex, as supported by the phase solubility profile. The presence of non-inclusion complexes, in addition to the inclusion complex, could not be ruled out and could account for the large excess of HPBCD needed to solubilise RTC1. The resultant complexes were characterized using analytical techniques such as SEM and DSC, while NMR spectroscopy allowed for the interaction to be investigated at a molecular level showing an interaction between RTC1 protons and internal protons of HPBCD. In vitro biological evaluation indicated that the RTC1/HPBCD complex showed comparable activity (ability to stimulate glucose uptake) to RTC1 alone, suggesting that RTC1 can disassociate from the CD and reach the target protein and hence improve bioavailability.

Supplementary data to this article can be found online at https://doi.org/10.1016/j.rechem.2020.100026.

Acknowledgements

The authors would like to thank Maynooth University, Government of Ireland Postgraduate Scholarship from the Irish Research Council, and Science Foundation Ireland TIDA grant number 08/IN.1/B1900 for funding. In addition, the authors thank Dr Padraig McLoughlin for his NMR assistance, Orla Fenelon for assistance with the SEM analysis, and Austin Power for his technical support.

References

[1] International Diabetes Federation Atlas 8th Edition2017.
[2] N.C.D.R.F. Collaboration, Lancet 387 (2016) 1513–1530.
[3] Y. Zheng, S.H. Ley, F.B. Hu, Nat. Rev. Endocrinol. 14 (2018) 88–98.
[4] C. Hu, W. Jia, Adv. Drug Deliv. Rev. 139 (2019) 3–15.
[5] P.T. Donnan, T.M. MacDonald, A.D. Morris, Diabet. Med. 19 (2002) 279–284.
[6] H. Florez, J. Luo, S. Castillo-Florez, G. Mitsi, J. Hanna, L. Tamariz, A. Palacio, S. Nagendran, M. Hagan, Postgrad. Med. 122 (2010) 112–120.
[7] D. Kirpichnikov, S.I. McFarlane, J.R. Sowers, Ann. Intern. Med. 137 (2002) 25–33.
[8] J. Wu, X. Luo, N. Thangthaeng, N. Sumien, Z. Chen, M.A. Rutledge, S. Jing, M.J. Forster, L.J. Yana, Biochem. Biophys. Rep. 11 (2017) 119–129.
[9] D.S.D. Martin, S. Leonard, R. Devine, C. Redondo, G.K. Kinsella, C.J. Breen, V. McEneaney, M.F. Rooney, T.S. Munsey, R.K. Porter, A. Sivaprasadarao, J.C. Stephens, J.B.C. Findlay, J. Mol. Endocrinol. 56 (2016) 261–271.
[10] D.G. Hardie, B.E. Schaffer, A. Brunet, Trends Cell Biol. 26 (2016) 190–201.
[11] S. Leonard, L.M. Tobin, J.B.C. Findlay, Eur. J. Pharmacol. 800 (2017) 1–8.
[12] Y. Rojas-Aguirre, L. Yépez-Mulia, I. Castillo, F. López-Vallejo, O. Soria-Arteche, A. Hernández-Campos, R. Castillo, F. Hernández-Luis, Bioorg. Med. Chem. 19 (2) (2011) 789–797.
[13] K.V. Sri, A. Kondaiah, J.V. Ratna, A. Annapurna, Drug Dev. Ind. Pharm. 33 (3) (2007) 245–253.
[14] M.V.G. de Araújo, E.K.B. Vieira, G.S. Lázaro, L. de Souza Conegero, O.P. Ferreira, L.S.E. Almeida, L.S. Barreto, N.B. da Costa Jr., I.F. Gimenez, Bioorg. Med. Chem. 15 (17) (2007) 5752–5759.
[15] S. Upadhye, S. Kulkarni, S. Majumdar, M. Avery, W. Gul, M. ElSohly, M. Repka, AAPS PharmSciTech 11 (2) (2010) 509–517.
[16] H.O. Ammar, H.A. Salama, M. Ghorab, A.A. Mahmoud, Int. J. Pharm. 309 (1–2) (2006) 129–138.
[17] R. Challa, A. Ahuja, J. Ali, R.K. Khar, AAPS PharmSciTech 6 (2) (2005) 329–357.
[18] T. Loftsson, M.E. Brewster, M. Másson, American Journal of Drug Delivery 2 (4) (2004) 261–275.
[19] L.X. Song, B.L. Li, R. Jiang, Chin. Chem. Lett. 8 (7) (1997) 1.
[20] T. Higuichi, K. Connors, Adv. Anal. Chem. Instrum. (1965) 117–210.
[21] T. Loftsson, M. Másson, M.E. Brewster, J. Pharm. Sci. 93 (5) (2004) 1091–1099.
[22] V. Gabelica, N. Galic, E. De Pauw, J. Am. Soc. Mass Spectrom. 13 (8) (2002) 946–953.

Update

Results in Chemistry

Volume 2, Issue , January 2020, Page

DOI: https://doi.org/10.1016/j.rechem.2020.100051

Results in Chemistry 2 (2020) 100051

Contents lists available at ScienceDirect

Results in Chemistry

journal homepage: www.elsevier.com/locate/rechem

Erratum regarding previously published articles in volume 2

The Declaration of Competing Interest statements were not included in the published version of articles that appeared in Volume 2 of *Results in Chemistry*. For the below articles, the authors declare that they have no known competing financial interests or personal relationships that could have appeared to influence the work reported in this paper.

NMR line-broadening and transverse relaxation time measurements support a di-radical intermediate for the reaction of chlorosulfonyl isocyanate with electron-rich alkenes (Volume 2, January 2020, 100015).

Allylic amination and carbon–carbon double bond transposition catalyzed by cobalt(II) azodioxide complexes (Volume 2, January 2020, 100016)

Investigating reaction pathways for formic acid and lignin at HTL conditions using ^{13}C-labeled formic acid and ^{13}C NMR (Volume 2, January 2020, 100019)

Removal of azoic dyes from aqueous solutions by chitosan enhanced ultrafiltration (Volume 2, January 2020, 100017)

Characterization of water hyacinth cellulose-g-poly(ammonium acrylate-*co*-acrylic acid)/nano-hydroxyapatite polymer hydrogel composite for potential agricultural application (Volume 2, January 2020, 100020)

Synthesis of zinc stannate nanoparticles by sol-gel method for photocatalysis of commercial dyes (Volume 2, January 2020, 100023).

Non-invasive optical micro-identification of ink verification in pen ink handwriting (Volume 2, January 2020, 100,025).

Characterization of an aryl piperazine/2-hydroxypropyl-β-cyclodextrin association, a complex with antidiabetic potential (Volume 2, January 2020, 100,026).

Detection of sparfloxacin based on water-soluble CuInS2 quantum dots (Volume 2, January 2020, 100027)

Application of the protoplast co-culture method for evaluation of allelopathic activities of volatile compounds, safranal and tulipalin A (Volume 2, January 2020, 100030).

Development of smartphone-based ECL sensor for dopamine detection: Practical approaches (Volume 2, January 2020, 100029).

Non-equilibrium steady state in closed system with reversible reactions: Mechanism, kinetics and its possible application for energy conversion (Volume 2, January 2020, 100031)

Synthesis of some new protic *N*1-Benzyl/Butyl-2-methyl-4-nitro-1*H*-imidazol-3-ium salts with 3,5-Diaminobenzoate, 3,5-Dinitrobenzoate, (*E*)-3-(4-Hydroxy-3-methoxyphenyl)acrylate and 2-Carboxy-5-nitrobenzoate as organic anions (Volume 2, January 2020, 100033)

NH4Cl Catalyzed synthesis of β-amino Esters (Volume 2, January 2020, 100036).

Large-scale removal of colloidal contaminants from artisanal wastewater by bipolar electrocoagulation with aluminum sacrificial electrodes (Volume 2, January 2020, 100,038).

Mechanochemical synthesis of some heterocyclic molecules using Sonogashira cross-coupling reaction and their anticancer activities (Volume 2, January 2020, 100037)

Adverse effect of synthesized Naringenin derivatives investigate with Zebrafish (*Danio rerio*) embryos (Volume 2, January 2020, 100039)

Catalyst-and organic solvent-free synthesis, structural, and theoretical studies of 1-arylidenamino-2,4-disubstituted-2-imidazoline-5-ones (Volume 2, January 2020, 100042)

New synthetic 1,2,4-triazole derivatives: Cholinesterase inhibition and molecular docking studies (Volume 2, January 2020, 100041)

Insights into features and lead optimization of novel type 1½ inhibitors of p38α mitogen-activated protein kinase using QSAR, quantum mechanics, bioisostere replacement and ADMET studies (Volume 2, January 2020, 100044)

https://doi.org/10.1016/j.rechem.2020.100051
2211-7156/© 2020 Published by Elsevier B.V.